Experimental evidence of structural transition at the crystal-amorphous interphase boundary between Al and Al_2O_3

2002 J. Phys.: Condens. Matter 14 1887

(http://iopscience.iop.org/0953-8984/14/8/316)

INSTITUTE OF PHYSICS PUBLISHING JOURNAL OF PHYSICS: CONDENSED MATTER

J. Phys.: Condens. Matter **14** (2002) 1887–1893 PII: S0953-8984(02)28084-4

Experimental evidence of structural transition at the crystal–amorphous interphase boundary between Al and Al_2O_3

Z Q Yang, L L He, S J Zhao and H Q Ye

Shenyang National Laboratory for Materials Science, Institute of Metal Research, Chinese Academy of Sciences, Shenyang 110016, People's Republic of China

E-mail: yangzq@imr.ac.cn

Received 20 August 2001
Published 15 February 2002
Online at stacks.iop.org/JPhysCM/14/1887

Abstract

High-resolution transmission electron microscopy observations on the structure of the interphase boundary between crystalline Al and amorphous Al_2O_3 coating reveal that an interfacial melting transition of Al occurs at 833 K, which is distinctly lower than the bulk melting point of Al. The crystalline lattice planes of Al near the interface bend or small segments of crystalline Al deviated from the matrix Al grains are formed. Stand-off dislocations formed at the interphase boundary are also observed. The amorphous Al_2O_3 coating plays an important role in retaining the evidence for structural transition at high temperature to room temperature, which makes it possible to make experimental observations.

1. Introduction

The role of crystalline defects, such as surfaces and interfaces, in melting of crystalline materials is well known [1,2]. On approaching the bulk melting temperature, a crystal surface undergoes an order–disorder transition that is called surface melting, and acts as the nucleation centre for the bulk melting process [3–5]. Moreover, because the atoms in the internal interface have a potential energy higher than that of the bulk atoms, the interface can become thermally disordered before the bulk. Because of the application of surface analysis techniques, such as low-energy electron diffraction (LEED) [6], core-level photoemission [4], medium-energy ion scattering (MEIS) [7] and extended x-ray absorption fine structure (EXAFS) [3, 8], surface premelting or melting has been widely studied by experimental observations. However, these techniques do not work in the field of interface transition. Therefore, most works in the field of interface transition have been carried out by molecular dynamics simulations in recent years [9–11].

0953-8984/02/081887+07$30.00

The external surfaces of crystals are more easily accessible experimentally than internal interfaces, such as grain boundaries, antiphase boundaries, crystal–crystal interphase boundaries and crystal–amorphous interphase boundaries. A rich and rapidly growing literature in both experiment and simulation has attested to the diversity of phase transition that surfaces might undergo. However, experimental knowledge of the phase equilibria of internal interfaces is much limited. Because of the importance of interfacial transitions for bulk defected materials, there is a great need for studies of the thermal disordering of interfaces.

Direct observations including transmission electron microscopy (TEM) and high-resolution TEM (HRTEM) have difficulty in giving detailed information at the atomic level of structural transition of surfaces and internal interfaces of crystalline bulk as the temperature is increased toward the bulk melting point for certain reasons. First, the thermal order–disorder transition of surfaces and interfaces is reversible, and the surface or interface disordering transition occurs upon heating at a certain temperature; however, the disordered layer recovers its original structure after cooling down. Therefore, no information about the disordered layer could be observed by examining the cooled samples. Second, the *in situ* observation of such thermal disordering at high temperature in TEM and HRTEM is not an easy technique to date. In other words, only if the microstructure of surface or interface melting were retained to room temperature could it be observed by HRTEM. In this paper, we report HRTEM observations of local structure of the interphase boundary between crystalline Al and the amorphous Al_2O_3 coating, which shed light on the structure transition induced by heating at the boundary.

Our research interest lies in the area of phase equilibria of crystal–amorphous interfaces. To date, few studies have been carried out on phase transitions of crystal–amorphous interfaces, even by molecular dynamics simulation. A metal nanoparticle shows a high tendency of passivation to form an oxide shell. For example, an amorphous aluminum oxide shell with thickness of 2–6 nm is formed on an Al particle by exposing it to air [12–15]. There are many crystal–amorphous interphase boundaries in bulk material consisting of such passivated metal particles, which offers a good chance of studying the phase transition of such an interface.

2. Experiment

Ultrafine Al powders were prepared by the active H_2 plasma evaporation method. Passivation was carried out by gradually exposing the Al powders to air, so as to form an Al_2O_3 shell which encapsulated the Al grains. The passivated powder was compacted into a disc with diameter of 25 mm and thickness of 1 mm, under a pressure of 1.42 GPa at room temperature. In order to study the influence of annealing temperature upon the microstructure evolution of the material, especially upon the interface between crystalline Al and the amorphous oxide shell, heat treatments of such cold-compacted discs were performed for 40 min in a vacuum anneal furnace with a vacuum of 5×10^{-3} Pa. The temperature of the heat treatment ranged from 623 to 933 K, and the rate of increase of temperature was 20 K min^{-1}. The annealed samples were cooled in air.

Thin foils for TEM and HRTEM observations were prepared as following. Small discs with 3 mm diameter were first punched out from the as-compacted or heat-treated samples; after that they were mechanically ground to 60 μm thick and then dimpled to 30 μm and finally ion milled. TEM and HRTEM observations were performed in a JEM2010 high-resolution electron microscope and HF2000 field emission gun TEM (FEGTEM), both operating at 200 kV. The point resolution of the JEM2010 and HF2000 are 0.19 and 0.24 nm, respectively. The x-ray energy dispersive spectrum (EDS) measurements were performed by Link Oxford equipment in the HF2000 FEGTEM. The probe size of the HF2000 is about 1 nm.

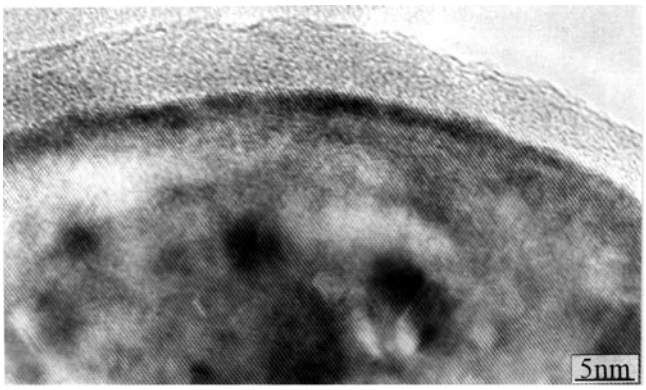

Figure 1. HRTEM image for the crystal/amorphous interface in one passivated Al particle in the cold-compacted sample.

3. Results and discussion

Figure 1 shows the HRTEM image for the interface region in one passivated Al particle in the cold-compacted sample. The lattice image of Al is sharp and continuous up to the crystal–amorphous interface. No obvious distortion of crystalline lattices of Al could be observed even near the interface. Therefore, even though an amorphous layer formed during passivation, it did not result in disordering of interior Al lattices during passivation. No dislocation can be seen in the Al crystal. It is noted that the interface is sharply defined but is not smooth on the atomic scale. In addition, TEM and HRTEM observations indicated that the crystal–amorphous interface structures of passivated Al particles in samples treated at 823 K and below for 40 min were the same as that shown in figure 1. That is, no structural reconstruction at the interface was observed in those samples annealed at 823 K and below.

Figure 2 shows the HRTEM image for the interface between crystalline Al and amorphous Al_2O_3 in the sample annealed at 833 K for 40 min. There is a step in the position indicated by 'A'. A metallurgical bond between the two adjacent Al grains at the atomic level was achieved on one side of the step to form an Al grain boundary. The contrast of the interface region on the other side of the step is ambiguous, but some segments of lattice fringes can be observed, and a brighter slice exists in the middle of the interface region. Nano-beam compositional analysis showed that there was Al oxide in the interfacial region (inset). From the EDS profile, the atomic ratio of Al:O is quantified to be 65:35, which suggests that this region is made of two phases, pure Al and Al_2O_3. It is known that amorphous phase does not show regular lattice fringes after the astigmatism is properly corrected. The HRTEM image of Al indicates that the astigmatism has been exactly corrected. Therefore, the boundary phase Al_2O_3 is amorphous according to the HRTEM image, which results in the blurring contrast. Measurement of lattice fringes in the interphase boundary region indicates that their interplanar spacing is equal to that of Al(111). According to the HRTEM image, the lattice fringes are not moiré patterns. Therefore, the lattice fringes in the interface region might come from crystalline Al. That is, small nuclei of Al were formed at the boundary upon heating at 833 K. The existence of a brighter slice without a lattice fringe in the middle of the interface region indicates that it is full of amorphous Al_2O_3. Some detailed information can be obtained by viewing along the arrows. First, the crystalline lattice planes of Al bend near the interface between crystalline Al and amorphous Al oxide, as indicated by black dots. However, no bending of Al crystalline lattice plane was observed at the grain boundary on the other side of the step. By comparing

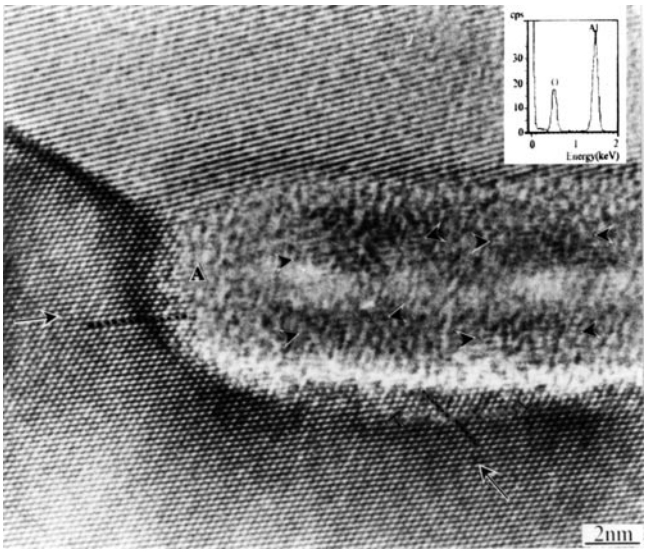

Figure 2. HRTEM image for the crystal/amorphous interface in the sample annealed at 833 K for 40 min.

with the crystal–amorphous interphase boundary in the cold-compacted sample (figure 1), the bending of Al crystalline lattice planes is the result of treating at 833 K. Second, there are edge dislocations within crystalline Al near the crystal–amorphous interphase boundary, as indicated by '⊥'. From the HRTEM image, the distance from the dislocation core to the interphase boundary is about 1 nm. There is another interpretation for the observed bending of Al crystalline lattice planes near the interphase boundary. That is, it may arise from change in thickness. However, the formation of dislocation must be a result of boundary structural transition, which on the other hand supports the proposal for the bending of lattice planes is induced by structural transition. It suggests that boundary structural transition occurred within a slab at least 1 nm during annealing at 833 K. Third, several segments of lattice fringe deviate from the both Al grains by misorientation of several degrees, as indicated by arrowheads. The deviation indicates those Al atoms under the amorphous Al_2O_3 rearranged too by treating at 833 K. Although no more dislocation besides those indicated by '⊥' can be distinguished from the HRTEM image, it can be reasonably deduced that there must be more dislocations at the boundary regions because of the misorientation between the small nuclei and the matrix grains of Al.

Figure 3 shows an HRTEM image for the crystal–amorphous interphase boundary region in the sample annealed at 893 K for 40 min. The upper part showing no regular crystalline lattice fringe is aluminum oxide, similar to that shown in figure 2. The arrowheads denote the position of the interphase boundary. It can be seen that the boundary is not flat at the atomic level. Two long white-edged arrows denote a crystalline defect within the crystalline Al phase. By viewing along the white arrow, it is found that the Al(111) planes on both sides of the defect indicated by arrows displace a little, as indicated by black dots. From the HRTEM image, the distance from the defect to the crystal–amorphous interphase boundary is about 3 nm. This suggests that a boundary structural transition occurred within a 3 nm thick slab of Al at least during annealing at 893 K. In addition, a dislocation with the extra atomic half plane of (002) and Burgers vector $a/2\langle 110\rangle$ was observed, as indicated by '⊥'. Moreover, the dislocation core was located on the arrow-indicated defect.

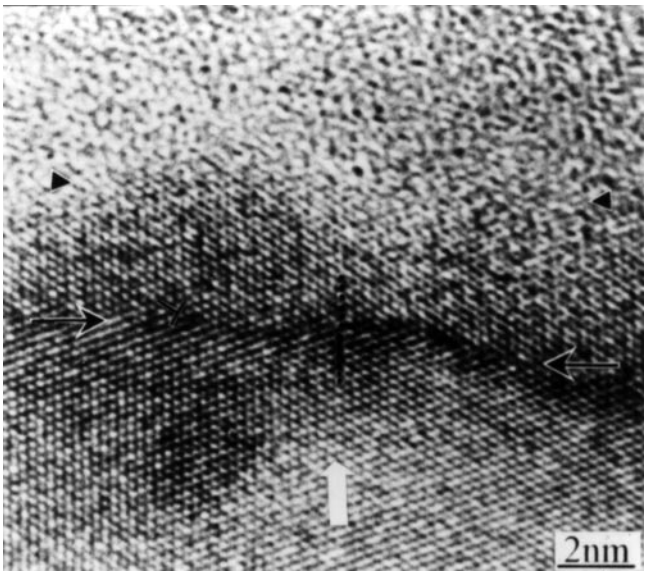

Figure 3. HRTEM image for the crystal/amorphous interface in the sample annealed at 893 K for 40 min.

Because initial crystals of Al were defect free (figure 1), any defect observed by HRTEM in samples annealed at temperature above 833 K can be attributed to the heat treatment process. In the temperature range from about 800 K up to the melting point (933 K) surface premelting and melting for Al have been observed by different experimental techniques. Molecular dynamics simulation on a $\Sigma = 5[001](\bar{1}30)$ symmetric tilt boundary of Al indicated that there was a melted interfacial layer with thickness of about 4 nm at 800 K [10]. Therefore, we might associate the change in crystalline lattice of Al and formation of dislocations in the interphase boundary region at and above 833 K with interface melting. The Al atoms in the layer near the interface form clusters, or rows and segments of them upon heating to a certain temperature, called thermal disordering [8–10], which destroys the long-range order in the lattice. Those clusters or segments of Al atoms can move with increased mobility to form a quasiliquid layer [16]. Because the melting point of Al_2O_3 is much higher than the annealing temperature, the Al_2O_3 layer must be solid during the annealing. Therefore, the interaction at the interface is that between the clusters of Al atoms and the solid amorphous Al_2O_3. Solidification of the quasiliquid layer of Al may begin at both quasiliquid–crystal and quasiliquid–amorphous interphase boundaries, similar to the cooling run in the grain boundary melting transition [10]. The formation of dislocation during the solidification of such a quasiliquid layer is readily explained. When growing surfaces of Al on both sides of the quasiliquid layer approach, there will be a driving force to form chemical bonds between atoms of opposing surfaces to achieve full coordination. However, surfaces are not flat at the atomic level so coherence will be achieved by distortion in some areas of the interface, and thus a dislocation will form [17]. According to simulation of a cooling run in a grain boundary melting transition, the quasiliquid–crystal interface grew in an epitaxial manner upon cooling. However, solidification on the side of a quasiliquid–amorphous interface was achieved by growth of random crystalline nuclei. Therefore, small Al crystallites appeared at the interface, as shown in figure 2. By comparing figures 2 and 3, it is found that the thickness of the structural transition layer in Al near the interphase boundary in the sample annealed at 893 K is about three times that in the sample

annealed at 833 K. This implies that the width of the structural transition (disorder) layer grows with temperature. This is consistent with other reports on surface (both experiment and calculation [1–8, 18]) and grain boundary (calculation [9–11]) melting. In short, because of the existence of the amorphous Al_2O_3 layer, the reversible transition of Al near the interface was interfered with. The evidence of partial order of the melted layer of Al was partly retained after cooling, which made it possible for HRTEM observation of such an interface. The grain boundary melting transition of Al might occur by annealing at 833 K and above. However, because the boundary layer recovered completely after cooling down to room temperature, no distortion of crystalline lattices could be observed with certainty. Therefore, the interaction at the crystal–amorphous interphase boundary is quite different from that at the crystal–crystal boundary.

Surface soft x-ray absorption spectroscopy implied that a nonstoichiometric and semiconducting oxide transition region should be present at the Al/Al_2O_3 interface [19]. HRTEM observations indicated that the transition region was at most two interplanar spacings wide, although Al had elastic and electrical properties quite different from those of Al_2O_3 [20]. Therefore, the Al/Al_2O_3 interface was sharply defined, as shown in figure 1. Neither stand-off misfit dislocation in Al nor a small nucleus of Al at the interphase boundary was reported even in a sample with a 100 nm thick Al_2O_3 coating formed at 673 K. Additionally, the difference in thermal expansion between Al and Al_2O_3 is less than 1% at 833 K [21,22]. Furthermore, no structural reconstruction at the boundary was observed in samples treated at 823 K, even though the difference in thermal expansion was also about 1% in these. Therefore, the generation of stand-off dislocations and small nuclei of Al at the boundary was probably not caused by the differential thermal expansion between the Al and Al_2O_3 or mixing of oxygen upon heating. On the other hand, strains induced by the differential thermal expansion between the Al and Al_2O_3 would be zero after cooling down to room temperature, which also indicated that the structural transition at the interphase boundary upon heating was not the result of the difference in thermal expansion between the Al and Al_2O_3.

It has been reported that an amorphous carbon matrix raised the melting temperature of tin microcrystals embedded in it [23]. Therefore, the amorphous Al_2O_3 coating might raise the transition temperature of the interface. This is probably the reason why structural transition at the interface was observed only in samples treated at 833 K and above.

Grain reorganization and lattice expansion have been observed in a number of nanocrystalline materials upon heating [24]. Our observations on the thermal reorganization of the Al/Al_2O_3 interface revealed the intrinsic character of another kind of structural transition. Although the structural transition occurred at the interface between crystalline Al and amorphous Al_2O_3, it must be a common property, which we believe holds for other kinds of internal interface.

4. Conclusions

In summary, we have observed some evidence for the structural transition at the crystal–amorphous interphase boundary in passivated Al nanoparticles. The structural transition is the result of thermal disordering, which is called interface premelting or melting. The amorphous Al_2O_3 played a key role in retaining the evidence for occurrence of interface premelting or melting, which made it possible to make HRTEM observations.

Acknowledgment

This work was supported by the National Natural Science Foundation of China (NSFC) under grant no 19874064 and 59895156.

References

[1] Cahn R W 1986 *Nature* **323** 668
[2] Cahn R W 1989 *Nature* **342** 619
[3] Polcik M, Wilde L and Haase J 1988 *Surf. Sci.* **405** 112
[4] Theis W and Horn K 1995 *Phys. Rev.* B **51** 7157
[5] Cheng H P and Berry R S 1992 *Phys. Rev.* A **45** 7969
[6] Prince K C, Breuer U and Bonzel H P 1988 *Phys. Rev. Lett.* **60** 1146
[7] Busch B W and Gustafsson T 2000 *Phys. Rev.* B **61** 16097
[8] Polcik M, Wilde L and Haase J 1997 *Phys. Rev. Lett.* **78** 491
[9] Zhao S J, Wang S Q, Zhang T G and Ye H Q 2000 *J. Phys.: Condens. Matter* **12** L549
[10] Nguyer T, Ho P S, Kwok T, Nitta C and Yip S 1986 *Phys. Rev. Lett.* **57** 1919
[11] Dymier P, Taiwo A and Kalonji G 1987 *Acta Metall.* **35** 2719
[12] Sánchez-López J C, González-Elipe A R and Fernández A 1998 *J. Mater. Res.* **13** 703
[13] Nieh T G, Luo P, Nellis W, Lesuer D and Benson D 1996 *Acta Mater.* **44** 3781
[14] Aumann C E, Skofronick G L and Martin J A 1995 *J. Vac. Sci. Technol.* B **13** 1178
[15] Sun X K, Cong H T, Sun M and Yang M C 2000 *Metall. Mater. Trans.* A **31** 1017
[16] Stoltze P, Norskov J K and Landman U 1989 *Surf. Sci.* **220** L693
[17] Lee Penn R and Banfield Jillian F 1998 *Science* **281** 969
[18] Barnet R N and Landman U 1991 *Phys. Rev.* B **44** 3226
[19] Bianconi A, Bachrach R Z, Hagstrom S B M and Flodstrom S A 1979 *Phys. Rev.* B **19** 2837
[20] Timsit R S, Waddington W G, Humphreys C J and Hutchison J L 1985 *Appl. Phys. Lett.* **46** 830
[21] *Handbook of Industrial Material* 1st edn (Trade and Technical) p 93
[22] Goldsmith A, Waterman T E and Hirschhorn H J 1961 *Handbook of Thermophysical Properties of Solid Materials* vol 3 p 45
[23] Allen G L, Gile W W and Jesser W A 1980 *Acta Metall.* **28** 1695
[24] Qin X Y, Wu X J and Cheng L F 1993 *Nanostruct. Mater.* **2** 99